JOURNAL OF Materials CHEMISTRY

Enhancement of photocurrent generation of two novel stilbazolium dye dimers in LB monolayer films

Fu-You Li,[a] Chun-Hui Huang,*[a] Lin-Pei Jin,*[b] Deng-Guo Wu[a] and Xin-Sheng Zhao[c]

[a]*State Key Laboratory of Rare Earth Materials Chemistry and Applications, Peking University–The University of Hong Kong Joint Laboratory on Rare Earth Materials and Bioinorganic Chemistry, Peking University, Beijing 100871, P. R. China*
[b]*Department of Chemistry, Beijing Normal University, Beijing 100875, China*
[c]*Department of Chemistry, Peking University, Beijing 100871, China*

Received 23rd April 2001, Accepted 10th September 2001
First published as an Advance Article on the web 16th October 2001

Novel amphiphilic stilbazolium dye dimers, bis{[1-(*N*-methylpyridinium-4-yl)-2-(3-methoxy-4-octadecyloxyphenyl)]ethenyl}methane diiodide (BPOM) and bis{[1-(*N*-methylpyridinium-4-yl)-2-(4-octadecyloxyphenyl)]ethenyl}methane diiodide (BPO) were synthesized, and they were successfully transferred onto semiconducting transparent indium–tin oxide (ITO) as H-aggregates by Langmuir–Blodgett (LB) techniques. The photocurrent generation properties of monolayer films of these dyes were investigated in a traditional three-electrode cell. A steady cathodic photocurrent was obtained upon excitation of the dye LB monolayer films deposited on an ITO electrode. The observed photocurrent generation quantum yield strongly depended on the applied electrode potential, concentration of the redox couples in the electrolyte solution, and the chemical structure of the dye congeners. The dye monomers, (*E*)-*N*-methyl-4-[2-(3-methoxy-4-octadecyloxyphenyl)ethenyl]pyridinium iodide (POM) and (*E*)-*N*-methyl-4-[2-(4-octadecyloxyphenyl)ethenyl]pyridinium iodide (PO) as the standards for comparison were also studied. Data show that the photocurrent generation quantum yields are 0.35% and 0.26% for BPOM and BPO, respectively, while those for POM and PO are 0.19% and 0.11%, respectively. From the photoelectrochemical measurement, the enhanced photocurrent generation properties in the dimer compared with those in the corresponding monomer were observed.

Introduction

It is known well that push–pull chromophores [*i.e.* molecules combining an electron-donating group (D) and an electron-accepting group (A) connected by a π conjugation system] are ideal nonlinear optical materials.[1,2] In previous publications, our group has found that Langmuir–Blodgett films of some D–π–A conjugated systems appended with strong electron donors and acceptors exhibit good photoelectric conversion properties.[3–13] Recently, our work indicates that better photocurrent generation of films can be observed when two or more chromophores are connected to one molecule by using suitable bridges.[8–13]

To explore the relationship of the chemical structure and photocurrent generation for the dimer and its monomer in more detail, herein we designed and synthesized two novel amphiphilic stilbazolium dye dimers linked together by a methylene group (CH_2), bis{[1-(*N*-methylpyridinium-4-yl)-2-(3-methoxy-4-octadecyloxyphenyl)]ethenyl}methane diiodide (BPOM) and bis{[1-(*N*-methylpyridinium-4-yl)-2-(4-octadecyloxyphenyl)]ethenyl}methane diiodide (BPO) (Scheme 1). The photoelectric conversion properties of indium–tin oxide (ITO) electrodes modified with LB monolayer films of these dyes were investigated. The possible mechanisms for photocurrent generation under different conditions are proposed.

Experimental

Materials

The stilbazolium dye dimers BPOM and BPO were prepared by the process shown in Scheme 2.

1,3-Di(pyridinium-4-yl)propane diiodide was prepared according to the previous method reported.[14] (3-Methoxy-4-octadecyloxy)benzaldehyde and 4-octadecyloxybenzaldehyde were synthesized as described in the literature.[15] The title dimer BPOM (or BPO) was synthesized by condensing 120.5 mg 1,3-di(pyridinium-4-yl)propane diiodide with 565.6 mg (3-methoxy-4-octadecyloxy)benzaldehyde (or 520.5 mg 4-octadecyloxy benzaldehyde) in absolute ethanol using piperidine as the catalyst. The product was purified by column chromatography on silica gel with a chloroform–methanol mixture (12 : 1) as the eluent.

BPOM: Yield: 31%. Mp: 196–198 °C. Anal. Calc. for

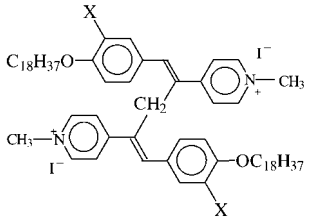

BPO X = H
BPOM X = CH_3O

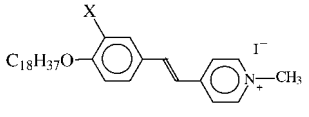

PO X = H
POM X = CH_3O

Scheme 1 The molecular structures of the materials BPOM and BPO.

 DOI: 10.1039/b103581a

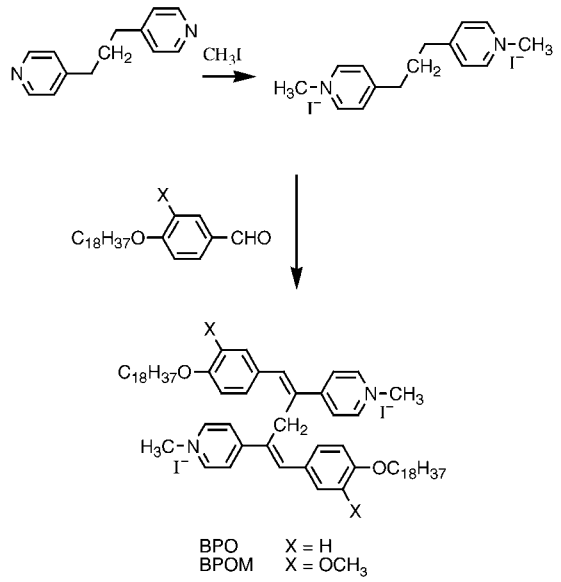

Scheme 2 The brief synthetic procedure for the compounds BPOM and BPO.

$C_{67}H_{104}N_2O_4I_2$: C, 64.10; H, 8.35; N, 2.23. Found: C, 63.88; H, 8.53; N, 2.01%. δ_H (300 MHz, $CDCl_3$): 0.88 (t, 6H, $2CH_3$), 1.26 (m, 60H, $2(CH_2)_{15}$),1.70–1.82 (m, 4H, $2CH_2$), 3.84 (s, 2H, =CH-CH_2-CH=), 4.04 (t, 4H, 2O-CH_2), 4.41 (s, 6H, $2N^+$-CH_3), 6.90 (m, 4H, Phenyl), 7.32–7.37 (m, 6H, Phenyl and 2CH=), 8.35 (m, 4H, pyridyl), 8.84 (m, 4H, pyridyl).

BPO: Yield: 37%. Mp: 201–203 °C. Anal. Calc. for $C_{65}H_{100}N_2O_2I_2$: C, 65.31; H, 8.43; N, 2.34. Found: C, 65.67; H, 8.10; N, 2.05%. δ_H (300 MHz, $CDCl_3$): 0.88 (t, 6H, $2CH_3$), 1.26 (m, 60H, $2(CH_2)_{15}$),1.70–1.82 (m, 4H, $2CH_2$), 3.80 (s, 2H, =CH-CH_2-CH=), 4.00 (t, 4H, 2O-CH_2), 4.18 (s, 6H, $2OCH_3$), 4.42 (s, 6H, $2N^+$-CH_3), 6.90 (m, 4H, Phenyl), 7.55 (d, 6H, Phenyl and 2CH=), 8.35 (m, 4H, pyridyl), 8.84 (m, 4H, pyridyl).

The stilbazolium dye monomers, (*E*)-*N*-methyl-4-[2-(3-methoxy-4-octadecyloxyphenyl)ethenyl]pyridinium iodide (POM) and (*E*)-*N*-methyl-4-[2-(4-octadecyloxyphenyl)ethenyl]-pyridinium iodide (PO) were synthesized by the previous method.[15] Methylviologen diiodide (MV^{2+}) was synthesized according to the previously reported method.[3] Hydroquinone (H_2Q), KCl and other reagents (Beijing Chemical Factory, China) were all analytical reagent grade and were used as received. $EuCl_3 \cdot 6H_2O$ was obtained by reaction of Eu_2O_3 with hydrochloric acid. The spreading solvent used for the monolayers deposition was chloroform (Beijing Chemical Factory, China). Water from a EASY pure RF system was used as a subphase ($R \approx 18$ MΩ cm, pH ≈ 5.6).

Apparatus

C, H, N data of the compounds were obtained by using a Carlo Erba 1106 elemental analyzer. ^{1}H NMR spectra were measured by using a Bruker ARX300. Electronic spectra in solution or on LB monolayer films were recorded on a Shimadzu model 3100 UV–Vis–NIR spectrophotometer. Melting points were performed on an X4 micromelting point apparatus. An automatic working NIMA 622 Langmuir–Blodgett trough with a Wilhelmy-type film balance was used for the measurement of surface pressure–area (π–A) isotherms and for the deposition of the monolayer LB films.

Pressure (π)–area (A) isotherm measurements and LB monolayer film formation

A sample of BPOM, BPO, POM and PO in chloroform solution (0.25 mg mL^{-1}) was spread onto a pure water subphase at 20 ± 1°C. After the evaporation of the solvent, the monolayer was compressed at a rate of 25 cm^2 min^{-1}, and then transferred at a rate of 5 mm min^{-1} (vertical dipping) under a surface pressure of 35 mN m^{-1}, onto ITO electrodes with a resistance of 250 Ω cm. To ensure the formation of the hydrophilic surface, the ITO electrode was immersed for 2 days in a saturated sodium methoxide solution in methanol and then thoroughly rinsed with pure water under ultrasonication several times. In all cases, the transfer ratios were close to 1.0 ± 0.1. Here, transfer ratio is defined as the ratio of the area of monolayer removed from the water surface to the area of substrate coated by the monolayer.

SHG measurement

The SHG measurements were performed in transmission geometry using a Y-type quartz plate ($d_{11} = 0.5$ pm V^{-1}) as a reference and with a Q-switched Nd : YAG laser (1.064 μm). A 1/2λ plate and a Glan–Taylor polarizer were used to vary the polarization direction of the laser beam. The laser light, linearly polarized either parallel (p) or perpendicular (s) to the plane of incidence, was directed at an incidence angle of 45° onto a vertically mounted sample. A set of 1.064 μm filters and a monochromator were used to ensure that the signal detected by the photomutiplier was the second-harmonic radiation generated by the films. The average output signal was recorded on a digital storage oscilloscope (HP54510). All the SHG data were averaged values of at least four individual measurements.

Photoelectrochemical measurements

A conventional glass three-electrode cell with the LB dye monolayer-modified ITO electrode (denoted as dye/ITO), platinum wire and saturated calomel electrode (SCE) as working electrode, counter electrode and reference electrode, respectively, was used in the measurements. The supporting electrolyte solution was 0.5 mol L^{-1} KCl aqueous solution in the photoelectrochemical studies. The effective area for illumination was 1.0 cm^2. The light source used for the photoelectrochemical study was a 500 W Xe arc lamp, the light beam was passed through a group of filters (*ca.* 300–800 nm, Toshiba Co., Japan, and Schott Co. Germany) in order to get a given bandpass of light. The light intensity at each wavelength was measured with an energy and power meter (Scientech Co., USA). Cyclic voltammetric (CV) experiments (sweep rate = 100 mV S^{-1}) were performed on an EG&GPAR 273 potentiostat/galvanostat with EG&GPAR 270 electrochemical software. Oxygen was removed from the electrolyte solution by bubbling N_2 for at least 15 min before every measurement.

Results and discussion

Properties of LB monolayer films

Fig. 1 shows the surface pressure–area (π–A) isotherms of the amphiphilic styryl dyes BPOM, BPO in the monolayer on the subphase. It can be seen from Fig. 1 that the collapse pressures of BPOM and BPO are 44.8 and 44.1 mN m^{-1}, respectively, which reveals that the two dyes have good film formation properties at the water/air interface. The molecular limiting area of BPO is 0.60 nm^2, extrapolated from the π–A curve under 35 mN m^{-1}. However, when the surface pressure continues to be increased, the isotherm of BPOM shows a plateau-like region from 0.64 nm^2 (25.8 mN m^{-1}) to 0.49 nm^2 (29.8 mN m^{-1}). The molecular limiting areas of BPOM are 0.74 and 1.20 nm^2, extrapolated from the π–A curve under 35 and 15 mN m^{-1} to zero, respectively.

Comparing the π–A isotherm of BPOM with that of BPO, it is known from Fig. 1 that below 20 mN m^{-1} surface pressure, the small solid phase slope of the BPOM π–A curve may be due

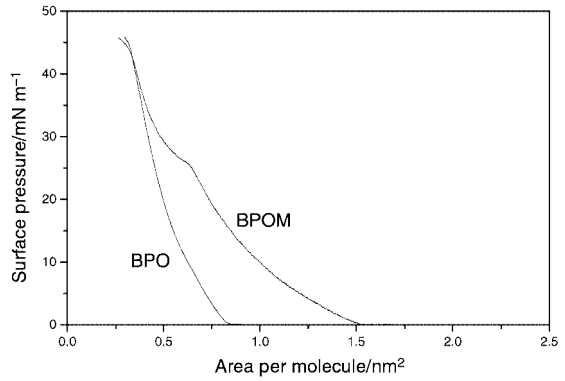

Fig. 1 The surface pressure *versus* area isotherms of BPOM and BPO at the air/water interface (20 ± 1 °C).

to the larger hydrophilic character of the oxygen atoms than those in the BPO molecule because there are four alkoxy groups in BPOM while BPO only has two alkoxy groups. The molecular limiting area of BPOM is larger than that of BPO, when extrapolated from the π–A curve below 35 mN m^{-1}; this is because there is a methoxy group on the third position of the phenyl ring.

It can be seen from Table 1 that the molecular limiting area of BPOM (or BPO) is smaller than twice that for POM (or PO) extrapolated from their π–A curves under 35 mN m^{-1}, which is in agreement with the fact that BPOM (or BPO) is a dimer derivative of POM (or PO). Therefore, we can conclude that the average density of chromophores in BPOM (or BPO) LB films is higher than that of POM (or PO), and that the average inter-chromophoric distance in BPOM (or BPO) is shorter than that in POM (or PO) assemblies.

To further understand the difference between the dimers and the monomers, the data from the UV–Vis spectra of BPOM, BPO, POM and PO in chloroform solution and on the LB films were also compared and are shown in Table 1. It can be seen from Fig. 2 that λ_{max} values for BPOM and BPO in chloroform solution are 402 and 380 nm, respectively. It is not difficult to understand that λ_{max} of BPOM in chloroform is 22 nm red-shifted relative to that of BPO because BPOM has four alkoxy groups as electron donors. When two D–π–A chromophores are linked together by a methylene group to form the BPOM and BPO molecules, the intramolecular and intermolecular interactions between the two D–π–A chromophores exist for BPOM and BPO in chloroform solution, whereas only intermolecular interaction exists for POM and PO in chloroform solution. Furthermore, from the molecular limiting area, the average inter-chromophoric distance in BPOM (or BPO) is shorter than that in POM (or PO) assemblies, which means that the average interaction between the π-orbits of the chromophores in BPOM (or BPO) becomes stronger than that of the

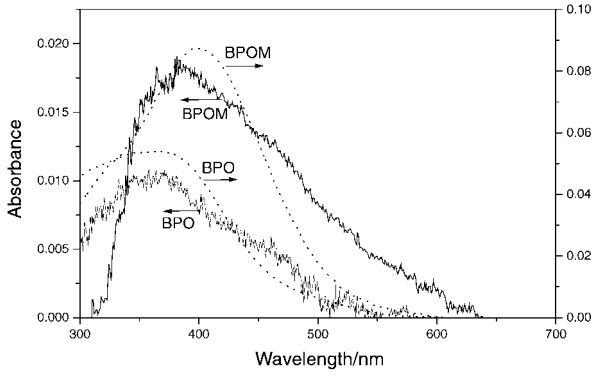

Fig. 2 UV–Vis absorption spectra of BPOM and BPO in chloroform solutions (···) and on LB monolayers (—).

Table 1 The properties of BPOM, BPO, POM and POM LB films

	Photocurrent I^a/nA cm^{-2}	Photocurrent I^b/nA cm^{-2}	External quantum yield η^b (%)	No. of molecules per cm^2 $No_{(m)}$/10^{14} cm^{-2}	Photocurrent per molecule I^{ad}/10^{-12} nA molecule^{-1}	Photocurrent I^c/nA cm^{-2}	External quantum yield η^c(%)	$\chi^{(2)}$/pm V^{-1}	φ^{d}/°	A^d/nm^2	$\lambda_{max(sol)}{}^d$/nm	$\lambda_{max(film)}{}^d$/nm
BPOM	~814	31	0.35	1.35	6.03	126	1.42	63	42	0.74	402	386
BPO	~348	13	0.26	1.67	2.08	42	0.86	45	36	0.60	380	371
POM	~260	11	0.19	2.38	1.09	32	0.55	41	39	0.42	376	370
PO	~187	8.2	0.11	2.86	0.65	21.5	0.29	32	35	0.35	360	356

[a]Under irradiation with 137.6 mW cm^{-2} white light for BPOM, BPO, POM and PO, in 0.5 mol L^{-1} KCl electrolyte solution under ambient conditions. [b]Under monochromized irradiation at 380 nm with 137.6 mW cm^{-2} white light for BPOM, BPO, POM and PO, in 0.5 mol L^{-1} KCl electrolyte solution under ambient conditions. [c]Under monochromized irradiation at 380 nm with 137.6 mW cm^{-2} white light for BPOM, BPO, POM and PO, at −100 mV and in 0.5 mol L^{-1} KCl solution under ambient conditions containing 5 mmol L^{-1} $EuCl_3$ and 4 mmol L^{-1} MV^{2+}. [d]φ: Tilt angle relative to the normal line on the substrate; A: limiting area per molecule; $\lambda_{max(sol)}$: absorption maximum of electric spectrum in chloroform solution; $\lambda_{max(film)}$: absorption maximum of electric spectrum for LB film.

chromophores in POM (or PO). Therefore, λ_{max} values for BPOM and BPO in chloroform are about 20 nm red-shifted compared with those of POM and PO.

In order to compare the efficiency of photocurrent generation, we chose the surface pressure of 35 mN m^{-1} as the condition for deposition of their LB monolayer films. Upon comparing the electronic spectra of LB monolayer films with those in chloroform (in Table 1, λ_{max}), blue-shifts of 16 and 9 nm can be observed for BPOM and BPO LB monolayer films, respectively, indicating that H-aggregates formed in the monolayer films for BPOM and BPO.[16]

SHG properties of the dyes films

On the assumption that the chromophores have a common tilt angle φ with respect to the normal of the film surface, with a random azimuthal distribution, and that the thickness of the monolayer (30 Å) for the dyes is calculated from the length of the molecule, the SHG data from the LB films were analyzed by the general procedure described by Ashwell *et al.*[17]

The second harmonic susceptibilities $\chi^{(2)}$ for BPOM and BPO LB monolayer films deposited on quartz under 35 mN m^{-1} are 63 and 45 pm V^{-1}, respectively, which are larger than those of POM (41 pm V^{-1}) and PO (32 pm V^{-1}) under the same conditions. λ_{max} values for BPOM and BPO in LB films are far from the resonance absorbance wavelength (532 nm), therefore the resonant enhancement effect of BPOM (or BPO) can be neglected. Therefore, we can conclude that the dimerization of D–π–A chromophores is favorable to an enhancement of the chromophore's SHG activity. It can be seen from Table 1 that the tilt angles φ of chromophores are 42 and 36° for BPOM and BPO LB monolayer films, respectively, relative to the normal of the substrate, which is similar to those obtained from films of the hemicyanine halides, such as PO (35°).[10,18] We can suggest that the possible orientation of BPO is as shown in Scheme 3. It is known that BPOM (or BPO) has a center of symmetry in the molecule when the two D–π–A chomophores take the *trans*-configuration relative to the CH_2 group (as shown in Scheme 1), and that cannot yield SHG according to the principle of second-harmonic nonlinear optics. In the solution, the BPOM (or BPO) molecule spends most of the time in non-centrosymmetric configurations due to molecular rotation, but the dipole moment is not large because the two D–π–A chromophores in one BPOM (or BPO) molecule take mostly partial *trans*-forms relative to the CH_2 group. At the water/air interface, the chromophores take almost the same orientation due to the existence of the hydrophobic tails and the hydrophilic heads. Therefore, the BPOM (or BPO) molecule has to take a non-centrosymmetric configuration, and the dipole moment in the LB film is enlarged; then the large second harmonic response is generated. This fact indicates that the LB technique can offer the opportunity to make the hydrophobic tails take the same direction, which benefits the formation of the non-centrosymmetric configuration.[19]

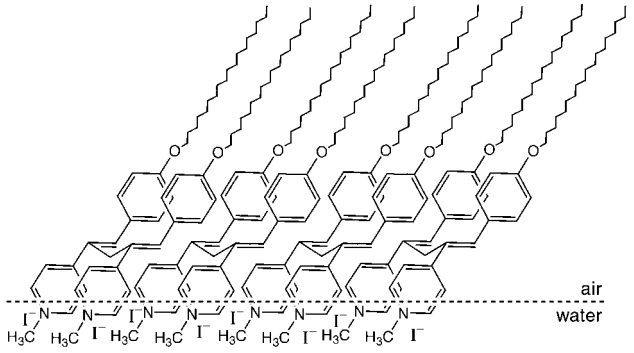

Scheme 3 The possible orientation of BPO at the water/air interface.

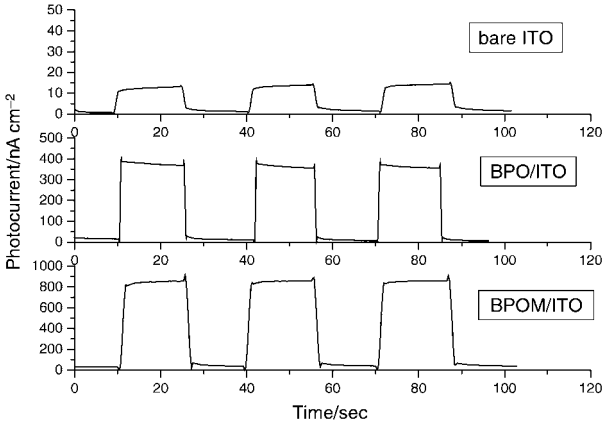

Fig. 3 The photoelectric responses of BPOM/ITO, BPO/ITO and bare ITO electrode, under irradiation with 137.6 mW cm^{-2} white light in 0.5 mol L^{-1} KCl electrolyte solution.

Photoelectric conversion properties

Upon irradiation with 137.6 mW cm^{-2} white light, steady cathodic photocurrents were observed from the BPOM and BPO monolayer film-modified ITO electrodes (denoted as BPOM/ITO and BPO/ITO, respectively) in 0.5 mol L^{-1} KCl solution (see Table 1, I^a). The photocurrent fell instantly when the illumination was cut off. The photoelectric responses of BPOM/ITO and BPO/ITO (for the examples) were shown in Fig. 3. However, the photocurrent generation of bare ITO electrode was very weak (see Fig. 3), which indicates that BPOM and BPO are dye sensitizers for the ITO electrode. Moreover, the action spectra of the cathodic photocurrent (see Fig. 4) are similar to their absorption spectra (see Fig. 2) from 300–800 nm for BPOM and BPO, suggesting that the BPOM/ITO and BPO/ITO monolayer films are responsible for photocurrent generation. About 31 nA cm^{-2} photocurrent can be obtained for BPOM/ITO on 380 ± 5 nm light irradiation which corresponds to an intensity of 1.36×10^{15} photons cm^{-2} s^{-1}, in 0.5 mol L^{-1} KCl electrolyte solution with zero bias voltage. The photocurrent generation quantum yield (η) was calculated according to eqns. (1) and (2):

$$\eta = i/[eI(1-10^{-A})] \quad (1)$$

$$I = W\lambda/hc \quad (2)$$

where i is observed photocurrent, e is the charge of the electron, I is the number of photons per unit area and unit time, A is the absorbance of the monolayer, λ is the wavelength of light irradiation, W is light power at λ nm, c is the light velocity, and h is Planck's constant. Therefore, the quantum yield is about

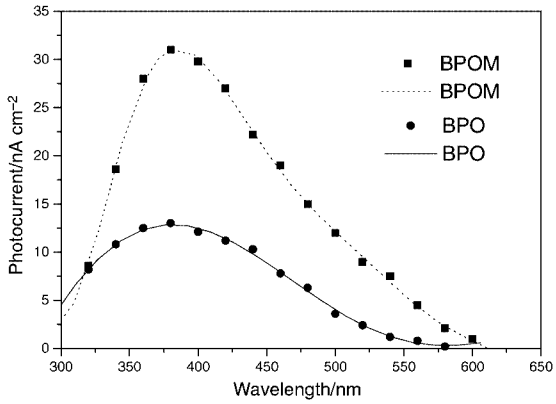

Fig. 4 The action spectra of the cathodic photocurrents for BPOM/ITO and BPO/ITO. The intensities of different wavelengths are all normalized.

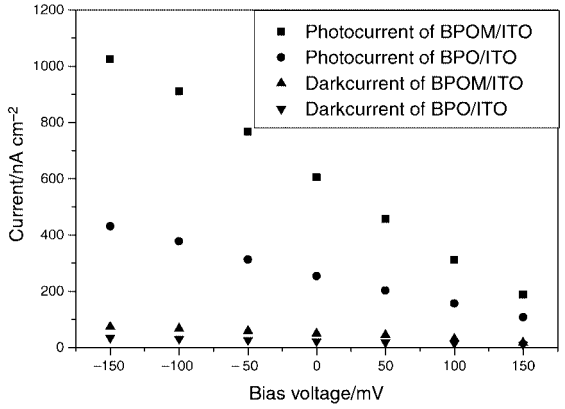

Fig. 5 Photocurrent and dark current for BPOM/ITO and BPO/ITO *versus* bias voltage in 0.5 mol L^{-1} KCl aqueous solution under ambient conditions, upon irradiation with 102 mW cm^{-2} white light.

0.35% for BPOM/ITO (in Table 1, η^b) (the absorbance of the monolayer films is about 0.018 at 380 nm), while those for BPO/ITO, POM/ITO and PO/ITO are 0.26%, 0.19% and 0.11%, respectively.

It is well known that the experimental conditions affect photocurrent generation sensitively. (1) In the range of +150 mV to −150 mV, a linear relationship was found between photocurrent and bias voltage whereas the dark current remains constant, as shown in Fig. 5, indicating that the photocurrent flows in the same direction as the applied negative voltage. (2) It can be seen from Fig. 6 that the equations of dependence of the photocurrent (i_{ph}) on light intensity (I) for BPOM/ITO and BPO/ITO are $i_{ph}=8.35\ I^{0.93}$ and $i_{ph}=4.19\ I^{0.88}$, respectively, while the photocurrent of the bare ITO electrode is very low. (3) The effects of electron donors (H_2Q and N_2) and acceptors (MV^{2+} and Eu^{3+}) on the cathodic photocurrent for BPOM/ITO (as an example in Table 2) and BPO/ITO show that electron acceptors sensitize the cathodic photocurrent and electron donors quench it (even reverse it). When air was removed from the solution by bubbling N_2, the cathodic photocurrents decrease greatly (see Table 2). On the other hand, the photocurrent increased by subsequent O_2 bubbling, and then recovered to the state under the air-saturated conditions. It is well known that O_2 acts as an electron acceptor in solution and can enhance the cathodic photocurrent generation in similar photoelectrochemical cells.[8,20] Addition of MV^{2+} into the solution could also increase the cathodic photocurrent (as shown in Fig. 7), because MV^{2+} can very easily accept an electron to form MV^{+} and accelerates the electron transfer from excited aggregates to the electrolyte solution.[20]

Under the optimal conditions (−100 mV, dissolved O_2, 5 mmol L^{-1} MV^{2+} and 4 mmol L^{-1} Eu^{3+}), we obtained a net photocurrent density of 124 nA cm^{-2} for BPOM/ITO upon irradiation at 380 ± 5 nm, and then the quantum yield of BPOM/ITO is 1.42%. Under the same conditions, the quantum yields of BPO/ITO, POM/ITO and PO/ITO are 0.86%, 0.55% and 0.26% (see Table 1, I^c, η^c), respectively.

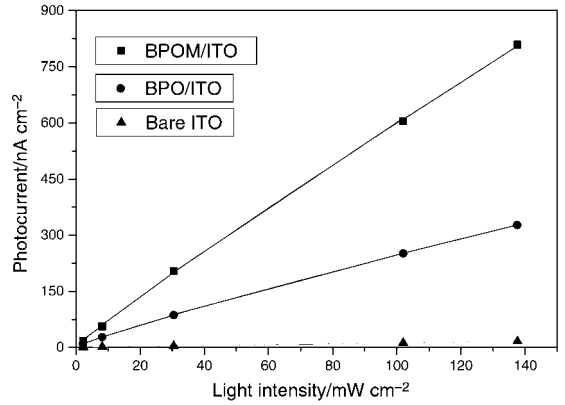

Fig. 6 Dependence of the photocurrent on light intensity for BPOM/ITO and BPO/ITO in 0.5 mol L^{-1} KCl electrolyte solution under ambient condition without bias voltage.

Table 2 Effect of donors and acceptors on the photoelectric conversion of BPOM/ITO

Donor/acceptor	Concn./mmol L^{-1}	Photocurrent[a]/nA cm^{-2}		
		Air	N_2	O_2
MV^{2+}	0	602	414	658
	4	1735	1325	1805
Eu^{3+}	0	620	420	685
	5	1215	795	1290
H_2Q	0	593	402	624
	5.4	−1564[b]	−2105[b]	−1380[b]

[a]Irradiation under 102 mW cm^{-2} white light for BPOM/ITO in 0.5 mol L^{-1} KCl electrolyte solution. [b]"−" indicates anodic photocurrent.

Mechanism of photoelectric conversion

To elucidate the mechanism of the photoinduced electron transfer process for the cathodic and anodic photocurrent, the energy levels of the relevant electronic states must be estimated. The oxidation peak potential for the dyes measured by the CV method provides a measurement of the energy of the HOMO. The oxidation peak potentials are 0.84 and 0.80 V for BPO/ITO and BPOM/ITO, respectively, and the energy levels of the excited state for BPO/ITO and BPOM/ITO are −5.58 eV (0.84 V *vs.* SCE) and −5.54 eV (0.80 V *vs.* SCE) on the absolute scale, respectively. With reference to UV–Vis spectra of BPO and BPOM LB monolayer films, their $\lambda_{max(film)}$ are 371 and 386 nm and their band gaps are 3.34 and 3.21 eV, respectively. Therefore, the energy levels of the ground state for BPO/ITO and BPOM/ITO are −2.24 and −2.33 eV on the absolute scale, respectively. The conduction band (E_c) and valence band (E_v) edges of the bare ITO electrode surface are estimated to be *ca.* −4.5 eV and −8.3 eV,[21] respectively. The reduction potential of MV^{2+} is −4.51 eV (−0.23 V *vs.* SCE),[20] reduction potential of Eu^{3+} is −4.39 eV (−0.35 V *vs.* SCE), and oxidation potential of H_2Q is −4.61 eV(−0.13 V *vs.* SCE),[21] on the absolute scale. Then, an energy level diagram for BPOM/ITO (as an example and as shown in Scheme 4) and BPO/ITO can be constructed.

From the above results, the photocurrent generation may be explained by the following mechanism, as shown in Scheme 4. It can be seen from the energy levels that the direction of the photocurrent depends not only on the dye sensitized by the light but also on the nature of the redox couple in the aqueous

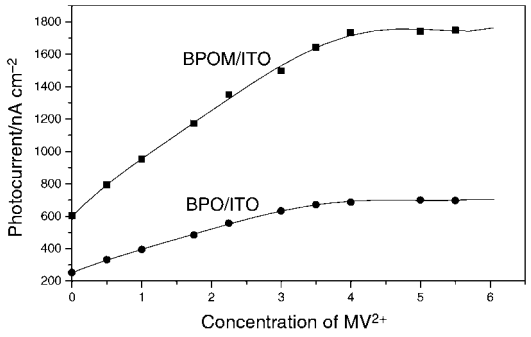

Fig. 7 Dependence of the photocurrent on the concentration of MV^{2+} under ambient conditions without bias voltage for BPOM/ITO and BPO/ITO upon irradiation with 102 mW cm^{-2} white light.

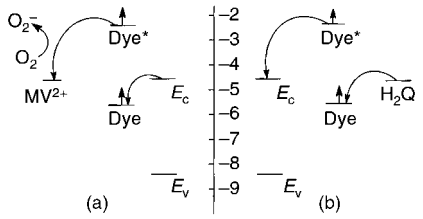

Scheme 4 Mechanism of electron transfer of the dye on ITO electrode in different conditions. (a) cathodic photocurrent; (b) anodic photocurrent. Dye and Dye* represent the ground state and the excited state of BPOM, respectively.

phase surrounding the electrode. In the presence of some electron acceptors, such as O_2, MV^{2+} and Eu^{3+} in electrolyte solution, electron transfer takes place from the excited state of BPOM (or BPO) to the electron acceptor, and subsequently the electrons of the ITO conduction band inject into the hole residing in the dye molecules. Thus, a cathodic photocurrent is generated. In contrast, if there is a strong electron donor in the system, such as H_2Q, it will exhibit a reduced photocurrent and even reverse the direction of photocurrent.

Correlation between molecular structure and PEC property

It can be seen from Table 1 that the photocurrent generation quantum yield of the dimer is higher than that of the monomer. One factor is that the average density of active D–π–A chromophores in the dimer is larger than in the monomer, because the number of active moieties per unit area in the LB monolayer films is an important factor contributing to the PEC performance. Here we use the photocurrent per chromophore as the basic data for comparison. To discuss it conveniently, we assume that BPO and BPOM contain two D–π–A chromophores. Taking the limiting molecular area into account, one can determine the molecular numbers per square centimetre as 1.35×10^{14}, 1.67×10^{14}, 2.38×10^{14} and 2.86×10^{14} for BPOM, BPO, POM and PO [Table 1, $No_{(m)}$], respectively. Consequently, the chromophore numbers per square centimetre for BPOM, BPO, POM and PO are 2.70×10^{14}, 3.34×10^{14}, 2.38×10^{14} and 2.86×10^{14}, respectively. Furthermore, with reference to the photocurrent per square centimetre, one can see that photocurrents per one molecule for BPOM, BPO, POM and PO are 6.03×10^{-12}, 2.08×10^{-12}, 1.09×10^{-12} and 6.5×10^{-13} nA molecule^{-1} (Table 1, I'^{a}), respectively. Therefore, the photocurrent generated by one BPOM molecule [6.03×10^{-12} nA (one BPOM molecule)$^{-1}$] is 2.77 times as large as the photocurrent generated by two POM molecules [$2\times1.09\times10^{-12}$ nA (two POM molecules)$^{-1}$], and the photocurrent generated by one BPO molecule [2.08×10^{-12} nA (one BPO molecule)$^{-1}$] is 1.6 times as large as the photocurrent generated by two PO molecules [$2\times6.5\times10^{-13}$ nA (two PO molecules)$^{-1}$]. That is, the photocurrent generated by one dimer molecule is larger than that of the two corresponding monomer molecules in LB films. Therefore, BPOM and BPO perform better in photocurrent generation than POM and PO do, respectively, which is not only due to their higher chromophore density of BPOM and BPO in LB films but also to the dimerization of the chromophores.

Conclusions

It can be seen from Table 1 that in the present systems the photocurrent generation quantum yield η of the dye LB monolayer has a sequence under the same conditions: BPO > PO and BPOM > POM, and that the dimers BPO and BPOM generate photocurrents of 2.08×10^{-12} nA molecule^{-1} for BPO and 6.03×10^{-12} nA molecule^{-1} for BPOM whereas the monomer PO generates a photocurrent of 0.65×10^{-12} nA molecules^{-1} and POM of 1.09×10^{-12} nA molecule^{-1}, when they are deposited on ITO electrodes under 35 mN m^{-1} by LB techniques. That is, the stilbazolium dye dimer exhibits an enhancement of photocurrent generation relative to the corresponding monomer. This is an interesting phenomenon of the dimer and monomer molecules. Thorough studies of the reason for this interesting phenomenon are in progress.

Acknowledgements

The authors thank the State Key Project of Fundamental Research (G1998061308) and National Natural Science Foundation of China (20023005, 59872001) and Doctoral Program Foundation of High Education (99000132) for financial support of this work.

References

1 H. S. Nalwa and S. Miyata, *Nonlinear Optics of Organic Molecules and Polymers*, CRC Press, Boca Raton, 1994.
2 D. R. Kanis, M. R. Ratner and T. J. Marks, *Chem. Rev.*, 1994, **94**, 195.
3 W. S. Xia, C. H. Huang, L. B. Gan and C. P. Luo, *J. Phys. Chem.*, 1996, **100**, 15525.
4 T. R. Cheng, C. H. Huang and L. B. Gan, *J. Mater. Chem.*, 1997, **7**, 631.
5 A. D. Liang, J. Zhai, C. H. Huang, L. B. Gan, Y. L. Zhao, D. J. Zhou and Z. D. Chen, *J. Phys. Chem. B*, 1998, **102**, 1424.
6 J. Zheng, C. H. Huang, T. X. Wei, Y. Y. Huang and L. B. Gan, *J. Mater. Chem.*, 2000, **10**, 921.
7 F. Y. Li, J. Zheng, L. P. Jin, C. H. Huang, Z. S. Wang and J. Q. Guo, *J. Colloid Interface Sci.*, 2000, **231**, 84.
8 C. H. Huang, F. Y. Li and Y. Y. Huang, *Ultrathin films for optics and electronics* (in Chinese), Peking University Press, Beijing, 2001.
9 D. G. Wu, C. H. Huang, L. B. Gan and J. Zheng, *Langmuir*, 1999, **15**, 7276.
10 D. G. Wu, C. H. Huang, L. B. Gan, W. Zhang, J. Zheng, H. X. Luo and N. Q. Li, *J. Phys. Chem. B*, 1999, **103**, 4377.
11 D. G. Wu, C. H. Huang, Y. Y. Huang and L. B. Gan, *J. Phys. Chem. B*, 1999, **103**, 7130.
12 F. Y. Li, J. Zheng, C. H. Huang, L. P. Jin, J. Y. Zhuang, J. Q. Guo, X. S. Zhao and T. T. Liu, *J. Phys. Chem. B*, 2000, **104**, 5090.
13 F. Y. Li, L. P. Jin, C. H. Huang, J. Zheng, J. Q. Guo, X. S. Zhao and T. T. Liu, *Chem. Mater.*, 2001, **13**, 192.
14 H. W. Gibson and F. C. Bailey, *J. Chem. Soc., Perkin Trans. 2*, 1976, 1575.
15 D. Lupo, W. Prass, U. Scheunemann, A. Laschewsky, H. Ringsdorf and I. Ledoux, *J. Opt. Soc. Am. B*, 1988, **5**, 300.
16 D. G. Whitten, *Acc. Chem. Res.*, 1993, **26**, 502.
17 G. J. Ashwell, P. D. Jackson, D. Lochum, W. A. Crossland, P. A. Thrompson, G. S. Bahra, C. R. Brown and C. Jasper, *Proc. R. Soc. London, Ser. A*, 1994, **445**, 385.
18 C. Bubeck, A. Laschewsky, D. Lupo, D. Neher, P. Ottenbreit, W. Paulus, W. Prass, H. Ringsdorf and G. Wegner, *Adv. Mater.*, 1991, **3**, 54.
19 G. J. Ashwell, G. Jefferies, D. G. Hamilton, D. E. Lynch, M. P. S. Roberts, G. S. Bahra and C. R. Brown, *Nature*, 1995, **375**, 385.
20 Y. S. Kim, K. Liang, K. Y. Law and D. G. Whitten, *J. Phys. Chem.*, 1994, **98**, 984.
21 L. Sereno, J. J. Silber, L. Otero, M. D. V. Bohorquez, A. L. Moore, T. A. Moore and D. Gust, *J. Phys. Chem.*, 1996, **100**, 814.